

User Selection Approaches to Mitigate the Straggler Effect for Federated Learning on Cell-Free Massive MIMO Networks

Tung T. Vu, Duy T. Ngo, Hien Quoc Ngo, Minh N. Dao, Nguyen H. Tran, and
Richard H. Middleton

Abstract

This work proposes UE selection approaches to mitigate the straggler effect for federated learning (FL) on cell-free massive multiple-input multiple-output networks. To show how these approaches work, we consider a general FL framework with UE sampling, and aim to minimize the FL training time in this framework. Here, training updates are (S1) broadcast to all the selected UEs from a central server, (S2) computed at the UEs sampled from the selected UE set, and (S3) sent back to the central server. The first approach mitigates the straggler effect in both Steps (S1) and (S3), while the second approach only Step (S3). Two optimization problems are then formulated to jointly optimize UE selection, transmit power and data rate. These mixed-integer mixed-timescale stochastic nonconvex problems capture the complex interactions among the training time, the straggler effect, and UE selection. By employing the online successive convex approximation approach, we develop a novel algorithm to solve the formulated problems with proven convergence to the neighbourhood of their stationary points. Numerical results confirm that our UE selection designs significantly reduce the training time over baseline approaches, especially in the networks that experience serious straggler effects due to the moderately low density of access points.

Index Terms

Cell-free massive MIMO, federated learning, user selection.

T. T. Vu, D. T. Ngo and R. H. Middleton are with the School of Electrical Engineering and Computing, The University of Newcastle, Callaghan, NSW 2308, Australia (e-mail: thanhtung.vu@uon.edu.au; {duy.ngo, richard.middleton}@newcastle.edu.au).

H. Q. Ngo is with the School of Electronics, Electrical Engineering and Computer Science, Queen's University Belfast, Belfast BT7 1NN, United Kingdom (e-mail: hien.ngo@qub.ac.uk).

N. H. Tran is with the School of Computer Science, The University of Sydney, Sydney, NSW 2006, Australia (e-mail: nguyen.tran@sydney.edu.au).

M. N. Dao is with the Centre for Informatics and Applied Optimization (CIAO), School of Engineering, Information Technology and Physical Sciences, Federation University, VIC 3350, Australia (e-mail: daonminh@gmail.com).

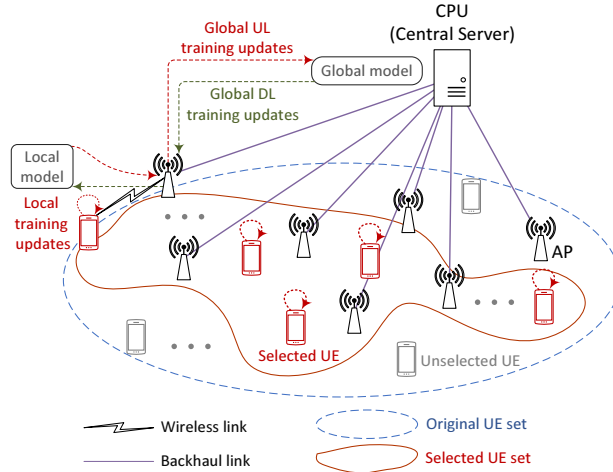


Fig. 1. A CFmMIMO network model with UE selection to support FL

I. INTRODUCTION

The numbers of mobile devices and connections have been growing significantly in recent years. According to Cisco [1], while the number of global mobile devices are expected to increase from 8.8 billion in 2018 to 13.1 billion by 2023, more than 10% of this number will have 5G connections. These devices are also generating a vast amount of data which can bring to mobile users (UEs) a wide range of on-device artificial intelligence (AI) services such as traffic navigation, indoor localization, image recognition, natural language processing, and augmented reality [2]–[4]. However, training AI models (especially by deep neural networks) at mobile devices using conventional centralized approaches in the current telecommunications systems is impractical. Such centralized system structures require a cloud center to store and process data, and thus, fails to support real-time applications because of their high latency. Moreover, uploading raw data to the cloud server raises serious concerns from mobile UEs about data privacy [5].

Federated learning (FL) has recently been emerged as an efficient solution to train AI models at mobile devices on wireless networks with a certain guarantee of data privacy [6]–[8]. With FL, the UEs compute their training updates using their local training data, and send the updates to a central server. These updates are aggregated by the central server to generate a global training update, which is then sent back to the UEs for the subsequent local computation. This iterative FL process terminates when a desired learning accuracy level is attained. Here, since only the training update (instead of the raw training data) is shared, the data privacy of each UE is protected. Moreover, because the size of a training update is much smaller than that of

the raw data, uploading only the training update would dramatically reduce the transmission delay. However, since the central server needs to wait for receiving the training updates from all the UEs participating in an FL process, the straggler UEs who have unfavorable links can significantly slow down the whole FL process. This is so-called “straggler effect”—the main bottleneck in realizing FL on wireless networks.

To mitigate the straggler effect, [9]–[11] propose FL frameworks that require only a subset of the UEs instead of all the UEs to send their local updates at each iteration of an FL process. The subset of UEs is chosen by specific sampling techniques so that the aggregation of training updates is unbiased and the FL process converges. Here, the network using UE sampling has a smaller probability of straggler UEs than that without using UE sampling. The straggler effect is thus mitigated in this sense. However, there is a chance that some of the sampled UEs are the straggler UEs. Therefore, using only UE sampling techniques is not always effective in mitigating the straggler effect.

On the other hand, [12]–[14] propose UE selection approaches to mitigate straggler effect. In particular, an online scheme that selects UEs in each iteration to minimize the training time while guaranteeing the convergence of the FL process is developed in [12]. A suboptimal scheme to jointly design bandwidth allocation and UE selection for training time minimization is devised in [13]. A novel FL framework with joint learning, resource block allocation, and UE selection scheme in order to minimize the training time while achieving a certain FL accuracy is introduced in [14]. However, realizing FL in time-division multiple access, frequency-division multiple access and orthogonal-frequency-division multiple access networks as [12]–[14] might not be efficient. The FL training time in such these networks could be significantly prolonged, especially when the number of UEs is large.

Very recently, cell-free massive multiple-input multiple-output (CFmMIMO) networks have been considered as a promising choice to support FL on wireless networks [15]. In a CFmMIMO network, the UEs are simultaneously served by a large number of distributed access points (APs) via wireless links using the same frequency band. The channel state information (CSI) is acquired via uplink (UL) training pilots. The APs are connected to a central processing unit (CPU) (i.e., the central server) via backhaul links. CFmMIMO networks offer high diversity, multiplexing, macro diversity gains, and hence, provide high-quality services to all the UEs [16]. More importantly, these networks offer channel hardening [17], i.e., the effective channels gains are reasonably stable in one large-scale coherence time. Using this characteristic, [15] proposes a framework

to implement FL so that each iteration of an FL process happens in one large-scale coherence time, and thus, the channel dynamics due to small-scale fading have negligible effects on the whole FL process. However, the straggler effect and the approaches to mitigate this effect for FL on CFmMIMO networks have not yet been investigated.

The contributions of this paper are summarized as follows.

- We propose, for the first time, UE selection approaches to mitigate the straggler effect for FL on CFmMIMO networks. To show how these approaches work, we consider a general FL framework with UE sampling [10], [11], and target FL training time minimization for this framework. Our approaches select a subset of UEs out of the original UEs before any FL process happens (as shown in Fig. 1). As such, they do not have any impact on the convergence of the FL process during the FL running time. They also have no requirement on the machine learning (ML) models. These properties make our approaches different from the existing UE selection methods in [12], [14] which select UEs at each iteration of the FL process and need to satisfy some strict requirements of the ML models to make sure the FL process eventually converges. Here, training updates are processed in three steps: (S1) the global training update is broadcasted to all the selected UEs from a central server; (S2) the local training updates are computed at the UEs; and (S3) sent back to the central server from the UEs sampled from the set of selected UEs.
- In our first and optimal UE selection approach, the time of one FL process is minimized by mitigating the straggler effects in both Steps (S1) and (S3). On the other hand, it can be observed that Step (S1) has a more serious straggler effect than Step (S3) since it does not have any UE sampling process. Therefore, we propose the second and suboptimal approach that minimizes the FL training time by mitigating only the straggler effect in Step (S1), and thus, has a lower complexity than the first approach. For these approaches, we formulate two mixed-integer two-stage stochastic nonconvex problems that capture the complex interactions among the training time, straggler effect, and UE selection. Here, we apply a conjugate beamforming/matched filtering scheme to the APs. This simple scheme can be implemented locally at each AP and performs well when the number of APs is large. The UE selection, power control, and data rate are jointly designed, subject to the practical constraints on the maximum powers at the APs and UEs, imperfect channel estimation, and the minimum number of UEs to guarantee the quality of learning.
- Using the general framework [18] for solving only two-stage stochastic nonconvex problems,

we propose a novel algorithm that is proven to converge to the neighbourhood of the stationary points of the formulated problems. Here, the binary nature of the UE selection variables and the coupling among the variables make it challenging to develop algorithms to solve the formulated problems. Such these algorithms need to handle the binary constraints efficiently as well as satisfies all the strict conditions stated in the general framework [18].

- Numerical results with practical settings verify the convergence of the proposed algorithms. They also show that our UE selection approaches reduce the training time by more than half compared to the baseline schemes, especially in the networks that have a low/moderate density of APs. Moreover, they confirm that the number of sampled UEs in Step (S3) and the minimum number of UEs to guarantee the quality of learning have noticeable impacts on the FL training time.

Notation: In this work, boldfaced symbols are used for vectors and capitalized boldfaced symbols for matrices. \mathbb{R}^d is a space where its elements are real vectors with length d . $\text{rnd}(x)$ is the nearest integer of x . \mathbf{X}^* and \mathbf{X}^H are the conjugate and conjugate transposition of a matrix \mathbf{X} , respectively. $\mathcal{CN}(\mathbf{0}, \mathbf{Q})$ denotes the circularly symmetric complex Gaussian distribution with zero mean and covariance \mathbf{Q} while $\mathcal{N}(0, V)$ the normal distribution with zero mean and variance V . ∇g is the gradient of a function g . $\mathbb{E}\{x\}$ denotes the expected value of a random variable x .

II. CELL-FREE MASSIVE MIMO SYSTEM MODEL TO SUPPORT WIRELESS FEDERATED LEARNING

A. The General FL Framework with UE Sampling [10], [11]

At a central server, a global ML problem is solved with a global training data set partitioned over a number of participating UEs. Each UE trains their local model by an arbitrary algorithm. Let N be the total number of UEs in the network. Denote by a_k an indicator variable that shows whether a user $k \in \mathcal{N} \triangleq \{1, \dots, N\}$ is selected to take part in an FL process or not, i.e.,

$$a_k \triangleq \begin{cases} 1, & \text{if UE } k \text{ is selected,} \\ 0, & \text{otherwise.} \end{cases} \quad (1)$$

Let $\tilde{\mathcal{N}}$ be the set of selected UEs to participate in an FL process, i.e.,

$$\tilde{\mathcal{N}} = \{k | a_k = 1, \forall k \in \mathcal{N}\}, \quad (2)$$

and $\tilde{N} \triangleq \sum_{k \in \mathcal{N}} a_k$ is the size of $\tilde{\mathcal{N}}$. Given the binary values of $\mathbf{a} \triangleq [a_1; \dots; a_N]$, (2) can be rewritten as:

$$\tilde{\mathcal{N}} \text{ is the index set of } \text{rnd}(\tilde{N}) \text{ largest elements from } \mathbf{a}. \quad (3)$$

Note that (3) is equivalent to (2) when the elements of \mathbf{a} are binary. When they are not binary, they can be considered as priority weights for UEs. In the latter case, (3) includes the UEs that have highest priority weights, and hence, is equivalent to (2) in this sense.

Let D_k be the size of the local data stored at UE k and $\tilde{D} = \sum_{k \in \tilde{\mathcal{N}}} D_k$ is the size of the global training data. Denote by $\mathcal{D} = \{1, \dots, \tilde{D}\}$ and $\mathcal{D}_k = \{1, \dots, D_k\}$ the index sets of the global data samples and the local data samples at a UE k , respectively. In a typical supervised learning, a data sample $i \in \mathcal{D}$ is defined as an input-output pair $\{\mathbf{x}_i, y_i\}$, where $x_i \in \mathbb{R}^d$, d is the length of the data vector, and $y_i \in \mathbb{R}$ or $\{-1, 1\}$. For $\lambda > 0$, the general global ML problem can be expressed as [10], [11]:

$$\min_{\mathbf{w} \in \mathbb{R}^d} J(\mathbf{w}) \triangleq \sum_{k \in \tilde{\mathcal{N}}} p_k f_k(\mathbf{w}), \quad (4)$$

where $p_k = \frac{D_k}{\tilde{D}} \geq 0$ is the weight of UE k and $\sum_{k \in \tilde{\mathcal{N}}} p_k = 1$. Here, $f_k(\mathbf{w})$ is the local cost function at UE k as

$$f_k(\mathbf{w}) \triangleq \frac{1}{D_k} \sum_{i \in \mathcal{D}_k} \tilde{f}_i(\mathbf{w}; (\mathbf{x}_i, y_i)), \quad (5)$$

where $\tilde{f}_i(\mathbf{w}; (\mathbf{x}_i, y_i))$ is the loss function at data sample i . The general FL framework with UE sampling [10], [11] is described in Algorithm 1. As can be seen, each iteration of Algorithm 1 includes the four steps (S1)-(S4).

B. CFmMIMO System Model to Support the General FL Framework with UE Sampling

We consider the CFmMIMO network model [15] illustrated in Fig. 1 to support the general FL framework with UE sampling discussed above. In this network model, a given set \mathcal{N} of UEs is served by a set of APs $\mathcal{M} = \{1, \dots, M\}$ via wireless access links at the same time and in the same frequency bands. The APs and UEs are each equipped with a single antenna. These APs are then connected to a central processing unit (CPU) via backhaul links with sufficient capacities. The CPU and UEs act as the central server and the clients in the general FL framework, respectively. Here, the APs relay the training updates between the CPU and the UEs.

Algorithm 1 A general FL framework with UE sampling [10], [11]

- 1: **Input:** $n = 1$, an initial global downlink (DL) training update
 - 2: **repeat**
 - 3: (S1) The central server sends the global DL training update to all \tilde{N} selected UEs, and choose a subset $\mathcal{S}^{(n)}$ of $K \leq \tilde{N}$ UEs randomly chosen with replacement according to the sampling probabilities $\{p_1, \dots, p_{\tilde{N}}\}$.
 - 4: **for** $k \in \mathcal{S}^{(n)}$ in parallel **do**
 - 5: (S2) UE k updates and solves its local ML problem (5) on its local data set and then computes the local UL training update
 - 6: (S3) UE k sends its computed local UL training update to the central server
 - 7: **end for**
 - 8: (S4) The central server computes the global DL training update by aggregating the received UL training updates.
 - 9: Update $n = n + 1$
 - 10: **until** convergence with the global accuracy ϵ
-

1) *UL channel estimation:* Denote by τ_c the number of samples of each coherence block. All the UEs send UL pilot sequences to all the APs simultaneously. Denote by τ_t (samples) the length of one pilot sequence. Let $\sqrt{\tau_t} \boldsymbol{\varphi}_k \in \mathbb{C}^{\tau_t \times 1}$ be the pilot sequence transmitted from UE $k \in \mathcal{N}$, where $\|\boldsymbol{\varphi}_k\|^2 = 1, \forall k \in \mathcal{N}$. The channel from a UE k to an AP m is modeled as

$$g_{mk} = (\beta_{mk})^{1/2} \tilde{g}_{mk}, \quad (6)$$

where β_{mk} and $\tilde{g}_{mk} \in \mathbb{C}$ represent the large-scale fading and small-scale fading channel coefficients, respectively. Assume that \tilde{g}_{mk} is a $\mathcal{CN}(0, 1)$ random variable.

The AP m receives the following pilot vector:

$$\mathbf{y}_m = \sqrt{\tau_t \rho_t} \sum_{k \in \mathcal{N}} g_{mk} \boldsymbol{\varphi}_k + \mathbf{w}_m, \quad (7)$$

where ρ_t is the normalized signal-to-noise ratio (SNR) of each pilot symbol, and $\mathbf{w}_m \in \mathcal{CN}(\mathbf{0}, \mathbf{I})$ is the additive noise at the AP m . The AP m estimates g_{mk} by using the minimum mean-square error (MMSE) estimation. Given \mathbf{y}_m , the MMSE estimate \hat{g}_{mk} of g_{mk} is obtained as [19]

$$\hat{g}_{mk} = \mathbb{E}\{\hat{y}_m^* g_{mk}\} (\mathbb{E}\{|\hat{y}_m|^2\})^{-1} \hat{y}_m = c_{mk} \hat{y}_m, \quad (8)$$

where $c_{mk} \triangleq \frac{\sqrt{\tau_t \rho_t} \beta_{mk}}{\sum_{\ell \in \mathcal{N}} \tau_t \rho_t \beta_{m\ell} |\boldsymbol{\varphi}_k^H \boldsymbol{\varphi}_\ell|^2 + 1}$, $\hat{y}_m \triangleq \boldsymbol{\varphi}_k^H \mathbf{y}_m = \sqrt{\tau_t \rho_t} \sum_{\ell \in \mathcal{N}} g_{m\ell} \boldsymbol{\varphi}_k^H \boldsymbol{\varphi}_\ell + \boldsymbol{\varphi}_k^H \mathbf{w}_m$ is the projection of \mathbf{y}_m onto $\boldsymbol{\varphi}_k$. Here, \hat{g}_{mk} is distributed according to $\mathcal{CN}(0, \sigma_{mk}^2)$, where $\sigma_{mk}^2 = \frac{\tau_t \rho_t (\beta_{mk})^2}{\sum_{\ell \in \mathcal{N}} \tau_t \rho_t \beta_{m\ell} |\boldsymbol{\varphi}_k^H \boldsymbol{\varphi}_\ell|^2 + 1}$ [19].

2) *Step (S1)*: The global DL training update intended for UE k is encoded into a symbol $s_{d,k} \sim \mathcal{CN}(0,1)$ at the CPU. The symbols $s_{d,k}, \forall k \in \mathcal{N}$ are then sent to all the APs over backhaul links. The APs use the channels obtained during the UL channel estimation phase to precode these symbols, and finally send the precoded versions to all the UEs. Let S_d (bits) and $R_{d,k}$ (bps) be the data size of the global DL training update and the data rate of sending the global DL training update to UE k , respectively. The DL transmission latency from the CPU to all the APs is given by

$$t_{d,B}(\mathbf{a}, \mathbf{R}_d) = \frac{\sum_{k \in \mathcal{N}} a_k S_d}{\sum_{k \in \mathcal{N}} a_k R_{d,k}}, \quad (9)$$

where $\mathbf{R}_d \triangleq [R_{d,1}; \dots; R_{d,N}]$, $\mathbf{a} \triangleq [a_1; \dots; a_N]$.

For ease of implementation, a conjugate beamforming scheme is applied to the APs to precode the message signals before these signals are transmitted to the UEs. The transmitted signal at an AP m is given as

$$x_{d,m} = \sqrt{\rho_d} \sum_{k \in \mathcal{N}} \sqrt{\eta_{mk}} (\hat{g}_{mk})^* s_{d,k}, \quad (10)$$

where ρ_d is the maximum normalized transmit power at each AP and $\eta_{mk}, \forall m \in \mathcal{M}, k \in \mathcal{N}$, is a power control coefficient. The transmitted power at AP m is required to meet the average normalized power constraint, i.e., $\mathbb{E}\{|x_{d,m}|^2\} \leq \rho_d$, which can be expressed as the following per-AP power constraint:

$$\sum_{k \in \mathcal{N}} \sigma_{mk}^2 \eta_{mk} \leq 1, \forall m. \quad (11)$$

The relation between a_k and η_{mk} is modeled as

$$\forall k \in \mathcal{N} : \text{if } a_k = 0, \text{ then } \forall m \in \mathcal{M}, \eta_{mk} = 0, \quad (12)$$

which means no power is allocated to the unchosen UEs.

The received signal at UE k is given by

$$\begin{aligned} r_{d,k} &= \sum_{m \in \mathcal{M}} g_{mk} x_{d,m} + w_k \\ &= \sqrt{\rho_d} \sum_{m \in \mathcal{M}} \sqrt{\eta_{mk}} g_{mk} (\hat{g}_{mk})^* s_{d,k} + \sqrt{\rho_d} \sum_{m \in \mathcal{M}} \sum_{\ell \in \mathcal{N} \setminus k} \sqrt{\eta_{m\ell}} g_{mk} (\hat{g}_{m\ell})^* s_{d,\ell} + w_k, \end{aligned} \quad (13)$$

$$h_{d,k}(\boldsymbol{\eta}) = \frac{\tau_c - \tau_t}{\tau_c} B \log_2 \left(1 + \frac{\rho_d \left(\sum_{m \in \mathcal{M}} \eta_{mk}^{1/2} \sigma_{mk}^2 \right)^2}{\rho_d \sum_{\ell \in \mathcal{N} \setminus k} \left(\sum_{m \in \mathcal{M}} \eta_{m\ell}^{1/2} \sigma_{m\ell}^2 \frac{\beta_{mk}}{\beta_{m\ell}} \right)^2 |\boldsymbol{\varphi}_\ell^H \boldsymbol{\varphi}_k|^2 + \rho_d \sum_{\ell \in \mathcal{N}} \sum_{m \in \mathcal{M}} \eta_{m\ell} \sigma_{m\ell}^2 \beta_{mk} + 1} \right) \quad (15)$$

where $w_k \in \mathcal{CN}(0, 1)$ is the additive noise at UE k . The achievable DL rate (bps) at UE k is

$$R_{d,k} \leq h_{d,k}(\boldsymbol{\eta}), \quad (14)$$

where $\boldsymbol{\eta} \triangleq \{\eta_{mk}\}_{m \in \mathcal{M}, k \in \mathcal{N}}$ and $h_{d,k}(\boldsymbol{\eta})$ is given in (15) shown at the top of the page [16], and B is the bandwidth. The DL transmission latency from the APs to UE k is given by

$$t_{d,k}(a_k, R_{d,k}) = \frac{a_k S_d}{R_{d,k}}. \quad (16)$$

3) *Step (S3)*: For given \mathbf{a} , let $\mathcal{S}^{(n)} \subset \tilde{\mathcal{N}}$ be the set of K UEs randomly selected from the set $\tilde{\mathcal{N}}$ of the selected UEs by the UE sampling techniques [10], [11]. Here, this set is chosen by randomly sampling UE with replacement according to the sampling probabilities $\{p_1, \dots, p_{\tilde{N}}\}$. Denote b_k by an indicator showing whether UE k is sampled or not, i.e.,

$$b_k \triangleq \begin{cases} 1, & \text{if } k \in \mathcal{S}^{(n)} \\ 0, & \text{otherwise,} \end{cases}, \forall k \in \mathcal{N}. \quad (17)$$

Note that for given \mathbf{a} , $\{b_k\}_{k \in \mathcal{S}^{(n)}}$ are constant.

After updating the local model, UE $k \in \mathcal{S}^{(n)}$ encodes the local UL training update into a symbol $s_{u,k} \sim \mathcal{CN}(0, 1)$. The symbol $s_{u,k}$ is then allocated a transmit amplitude value $\sqrt{\rho_u \zeta_k}$ to generate a baseband signal $x_{u,k}$ for wireless transmissions, i.e., $x_{u,k} = \sqrt{\rho_u \zeta_k} s_{u,k}$. UE k is subjected to the average transmit power constraint, i.e., $\mathbb{E}\{|x_{u,k}|^2\} \leq \rho_u$, which can also be expressed in a per-UE constraint as

$$0 \leq \zeta_k \leq 1, \forall k \in \mathcal{N}. \quad (18)$$

Since $\{b_k\}_{k \in \mathcal{S}^{(n)}}$ are only chosen if \mathbf{a} is known, the relation between a_k , b_k and ζ_k is modeled as

$$\forall k \in \mathcal{N} : \text{if } a_k b_k = 0, \text{ then } \zeta_k = 0, \quad (19)$$

which means no power is allocated to the unsampled UEs. The UL transmission latency from

$$h_{u,k}(\zeta) = \frac{\tau_c - \tau_t}{\tau_c} B \log_2 \left(1 + \frac{\rho_u \zeta_k (\sum_{m \in \mathcal{M}} \sigma_{mk}^2)^2}{\rho_u \sum_{\ell \in \mathcal{N} \setminus k} \zeta_\ell \left(\sum_{m \in \mathcal{M}} \sigma_{mk}^2 \frac{\beta_{m\ell}}{\beta_{mk}} \right)^2 |\boldsymbol{\varphi}_k^H \boldsymbol{\varphi}_\ell|^2 + \rho_u \sum_{\ell \in \mathcal{N}} \zeta_\ell \sum_{m \in \mathcal{M}} \sigma_{mk}^2 \beta_{m\ell} + \sum_{m \in \mathcal{M}} \sigma_{mk}^2} \right) \quad (25)$$

UE $k \in \mathcal{S}^{(n)}$ to the APs is given by

$$t_{u,k}(a_k, R_{u,k}) = \frac{a_k b_k S_u}{R_{u,k}}, \quad (20)$$

where S_u (bits) and $R_{u,k}$ (bps) are the data size of the local UL training updates and the data rate of transmitting the local UL training update from UE k to the CPU, respectively. Here, we assume that S_u is the same for all the UEs.

The received signal at AP m is expressed as:

$$y_{u,m} = \sum_{k \in \mathcal{N}} g_{mk} x_{u,k} + w_{u,m} = \sqrt{\rho_u} \sum_{k \in \mathcal{N}} g_{mk} \sqrt{\zeta_k} s_{u,k} + w_{u,m}, \quad (21)$$

where $w_{u,m} \sim \mathcal{CN}(0, 1)$ is the additive noise. To detect the message symbol transmitted from UE k , AP m computes and sends $(\hat{g}_{mk})^* y_{u,m}$ to the CPU. The UL transmission latency from the APs to the CPU is expressed as

$$t_{u,B}(\mathbf{a}, \mathbf{R}_u) = \frac{\sum_{k \in \mathcal{N}} a_k b_k S_u}{\sum_{k \in \mathcal{N}} a_k b_k R_{u,k}} \quad (22)$$

where $\mathbf{R}_u \triangleq [R_{u,1}; \dots; R_{u,N}]$.

At the CPU, the symbol $s_{u,\ell}$ is detected from the received signal $r_{u,k}$:

$$r_{u,k} = \sqrt{\rho_u} \sum_{m \in \mathcal{M}} \sqrt{\zeta_k} (\hat{g}_{mk})^* g_{mk} s_{u,k} + \sqrt{\rho_u} \sum_{m \in \mathcal{M}} \sum_{\ell \in \mathcal{N} \setminus k} \sqrt{\zeta_\ell} (\hat{g}_{mk})^* g_{m\ell} s_{u,\ell} + \sum_{m \in \mathcal{M}} (\hat{g}_{mk})^* w_{u,m}. \quad (23)$$

The achievable UL rate for the UE k is given by

$$R_{u,k} \leq h_{u,k}(\zeta), \quad (24)$$

where $\zeta \triangleq \{\zeta_k\}_{k \in \mathcal{N}}$ and $h_{u,k}(\zeta)$ is defined in (25) shown at the top of the next page [16].

III. PROBLEM FORMULATIONS

In this section, we first show how the straggler effect happens in Steps (S1) and (S3) of the FL process. We then aim to choose $\tilde{N} \geq K$ UEs out of the original N UEs to achieve the lowest

FL training time.

The transmission time of Step (S1) involves the DL transmission delay of sending the global DL training update from the CPU to the APs via backhaul links and that from the APs to all the UEs via wireless links, i.e.,

$$T_d(\mathbf{a}, \mathbf{R}_d) = t_{d,B}(\mathbf{a}, \mathbf{R}_d) + \max_{k \in \mathcal{N}} t_{d,k}(a_k, R_{d,k}) = \frac{\sum_{k \in \mathcal{N}} a_k S_d}{\sum_{k \in \mathcal{N}} a_k R_{d,k}} + \underbrace{\max_{k \in \mathcal{N}} \frac{a_k S_d}{R_{d,k}}}_{\text{Straggler effect in Step (S1)}}. \quad (26)$$

Similarly, the transmission time of Step (S3) consists of the delay of transmitting the global UL training update from the UEs to the APs and that from the APs to the CPU, i.e.,

$$T_u(\mathbf{a}, \mathbf{R}_u) = \max_{k \in \mathcal{N}} t_{u,k}(a_k, R_{u,k}) + t_{u,B}(\mathbf{a}, \mathbf{R}_u) = \underbrace{\max_{k \in \mathcal{N}} \frac{a_k b_k S_u}{R_{u,k}}}_{\text{Straggler effect in Step (S3)}} + \frac{\sum_{k \in \mathcal{N}} a_k b_k S_u}{\sum_{k \in \mathcal{N}} a_k b_k R_{u,k}}. \quad (27)$$

Therefore, the transmission time of one iteration of the FL process is

$$T_o(\mathbf{a}, \mathbf{R}_d, \mathbf{R}_u) = T_d(\mathbf{a}, \mathbf{R}_d) + T_u(\mathbf{a}, \mathbf{R}_u). \quad (28)$$

Note that, in (26) and (27), the terms of straggler effect can be much larger than the remaining terms, especially when there are UEs that have highly favorable links in a network having a large number of UEs. (26) and (27) imply that the straggler effect could lead to a long transmission time of each iteration of an FL process in (28). On the other hand, that UE selection has impacts on power control via (12) and (19), and thus, also affect the rates via (14) and (24). Therefore, to reduce the straggler effect as well as to minimize the transmission time of one iteration of the FL process, a joint optimization of UE selection, power control, and rates is necessary. It should also be noted in (27) that since the sampled UEs are always in the set of the selected UEs with favorable links, mitigating the straggler effect by both UE selection and sampling is more efficient than that by UE sampling alone.

As seen from (28), $T_o(\mathbf{a}, \mathbf{R}_d, \mathbf{R}_u)$ depends on both \mathbf{a} (UE selection) and \mathbf{R}_d (rate allocation). However, the UEs must be selected before any FL process is executed, while the rates are optimized before each iteration of the FL process happens. Because of this, to measure how efficiently the transmission time is optimized, we introduce a new metric termed ‘‘ergodic or effective transmission time of one iteration of an FL process’’, i.e., $T_e \triangleq \mathbb{E}\{T_o(\mathbf{a}, \mathbf{R}_d, \mathbf{R}_u)\}$. Since each iteration of the FL process happens in one large-scale coherence time, $\mathbb{E}\{T_o(\mathbf{a}, \mathbf{R}_d, \mathbf{R}_u)\}$ is, therefore, the average of $T_o(\mathbf{a}, \mathbf{R}_d, \mathbf{R}_u)$ over the large-scale fading realizations.

Let G be the number of iterations of an FL process. Let $T_c(\mathbf{a}, t_{c,k}) = \max_{k \in \mathcal{N}} a_k t_{c,k}$ be the computation time at Step (S2) at each iteration of an FL process, where $t_{c,k}$ is the time of computing the local UL training update at UE k . The effective training time of one FL process is given by

$$T_{e,\text{total}} = G \times (\mathbb{E}\{T_o(\mathbf{a}, \mathbf{R}_d, \mathbf{R}_u)\} + \mathbb{E}\{T_c(\mathbf{a}, t_{c,k})\}). \quad (29)$$

Here, we note that G is different for different ML models. G is known at some specific types of cost functions $J(\mathbf{w})$ but these cost functions must satisfy strict conditions such as [10, Assumptions 1, 2] and [11, Assumptions 1, 2]. Moreover, G is usually unknown for complicated and nonconvex $J(\mathbf{w})$ in complex ML models such as deep neural networks. Therefore, for the sake of generality, in this work, G is considered a constant as an upper bound of the number of iterations of an FL process. It should be noted that in the literature, G is also normally fixed when comparing the performances of different FL frameworks [10]. On the other hand, reducing the computation time T_c requires a strict coordination among all the UEs to adjust the local processing frequencies and the number of local iteration, which may be impossible in practice. Therefore, in this work, we focus only on minimizing the transmission time by mitigating the straggler effect at Steps (S1) and (S3). Here, we assume T_c is a constant as an upper bound of the computation time at each iteration of one FL process.

Since G and T_c are fixed, the problem of FL training time minimization is now expressed as

$$\min_{\mathbf{a}, \boldsymbol{\eta}, \boldsymbol{\zeta}, \mathbf{R}_d, \mathbf{R}_u} T_e(\mathbf{a}, \mathbf{R}_d, \mathbf{R}_u) \triangleq \mathbb{E}\{T_o(\mathbf{a}, \mathbf{R}_d, \mathbf{R}_u)\} \quad (30a)$$

$$\text{s.t. (1), (11), (12), (14), (18), (19), (24)}$$

$$0 \leq \eta_{mk}, \forall m, k \quad (30b)$$

$$0 \leq \zeta_k, \forall k \quad (30c)$$

$$0 \leq R_{d,k}, \forall k \quad (30d)$$

$$0 \leq R_{u,k}, \forall k \quad (30e)$$

$$\sum_{k \in \mathcal{N}} a_k \geq N_{\text{QoL}}, \quad (30f)$$

where $N_{\text{QoL}} \geq K$ is a threshold to ensure the *quality of learning*. The quality of a statistical learning scheme such as FL is defined as the test accuracy obtained after running that scheme.

It can be shown in [20] that the test accuracy of FL becomes worse if a number of UEs that are selected to participate in an FL process decreases. In (30f), the quality of FL is thus guaranteed by keeping the number of UEs participating in an FL process to be larger than a certain value N_{QoL} . In practice, N_{QoL} is experimentally chosen according to specific ML models.

Problem (30) has a nonconvex stochastic, mixed-integer mixed-timescale structure, along with the binary constraints and the tight coupling among the variables. Finding its globally optimal solution is challenging. This paper instead aims to propose a solution approach that is suitable for practical implementation.

Remark 1. It can be shown in [11] that *the convergence rate of federated learning with descent methods does not rely on the total number \tilde{N} of participating UEs but the number K of sampled UEs*. Therefore, selecting \tilde{N} UEs out of the original N UEs does not affect the convergence rate of the FL framework in [11]. This also means the problem (30) is general and can be used not only for the cost functions with an unknown G but also the cost functions that offer a known G and satisfy conditions [11, Assumptions 1, 2].

Remark 2. In cases that the ML models provide G that can be written as a function $G(\mathbf{a})$ of \mathbf{a} (UE selection) and the computation time $T_c(\mathbf{a}, t_{c,k})$ is taken into account, the total training time minimization problems can be expressed as slightly modified versions of (30) with the cost function (30a) replaced by $\tilde{T}_e(\mathbf{a}, \mathbf{R}_d, \mathbf{R}_u) \triangleq (\mathbb{E}\{G(\mathbf{a})T_o(\mathbf{a}, \mathbf{R}_d, \mathbf{R}_u)\} + \mathbb{E}\{G(\mathbf{a})T_c(\mathbf{a}, t_{c,k})\})$. Here, \tilde{T}_e involves variables that are optimized in different timescales as T_e . The UE selection variables \mathbf{a} are optimized in long-term timescales while the remaining variables such as power, rates, and computation time are optimized in short-term timescales. In this sense, the mixed-integer mixed-timescale stochastic structures of these problems are the same as that of (30). Therefore, we use the problem (30) to represent this structure without loss of generality. Moreover, the structure of the algorithms to solve these problems is also the same as that developed in the next section.

IV. PROPOSED ALGORITHM

First, to deal with the binary constraint (1), we observe that $x \in \{0, 1\} \Leftrightarrow x \in [0, 1] \ \& \ x - x^2 \leq 0$ [21], [22]. Therefore, problem (30) is equivalent to

$$\min_{\mathbf{a}, \boldsymbol{\eta}, \boldsymbol{\zeta}, \mathbf{R}_d, \mathbf{R}_u} \mathbb{E}\{T_o(\mathbf{a}, \mathbf{R}_d, \mathbf{R}_u)\} \quad (31a)$$

$$\text{s.t. (11), (12), (14), (18), (19), (24), (30b) – (30f)}$$

$$\sum_{k \in \mathcal{N}} (a_k - a_k^2) \leq 0 \quad (31b)$$

$$0 \leq a_k \leq 1, \forall k. \quad (31c)$$

We then rewrite the main problem (31) in an epigraph form as

$$\min_{\mathbf{x}} \mathbb{E} \left\{ \frac{\sum_{k \in \mathcal{N}} a_k S_d}{\sum_{k \in \mathcal{N}} a_k R_{d,k}} + t_d + t_u + \frac{\sum_{k \in \mathcal{N}} a_k b_k S_u}{\sum_{k \in \mathcal{N}} a_k b_k R_{u,k}} \right\} \quad (32a)$$

$$\text{s.t. (11), (12), (14), (18), (19), (24),}$$

$$(30b) - (30f), (31b), (31c)$$

$$\frac{a_k S_d}{R_{d,k}} \leq t_d, \forall k \quad (32b)$$

$$\frac{a_k b_k S_u}{R_{u,k}} \leq t_u, \forall k, \quad (32c)$$

where $\mathbf{x} \triangleq \{\mathbf{a}, \boldsymbol{\eta}, \boldsymbol{\zeta}, \mathbf{R}_d, \mathbf{R}_u, t_d, t_u\}$; t_d and t_u are additional variables. According to [23], problem (32) can be decomposed into a family of short-term subproblems and a long-term master problem as follows.

For a given \mathbf{a} , in each large-scale coherence time, the *short-term subproblem* is expressed as:

$$\min_{\tilde{\mathbf{x}}} \frac{\sum_{k \in \mathcal{N}} a_k S_d}{\sum_{k \in \mathcal{N}} a_k R_{d,k}} + t_d + t_u + \frac{\sum_{k \in \mathcal{N}} a_k b_k S_u}{\sum_{k \in \mathcal{N}} a_k b_k R_{u,k}} \quad (33)$$

$$\text{s.t. (11), (12), (14), (18), (19), (24), (30b) - (30e), (32b), (32c),}$$

where $\tilde{\mathbf{x}} \triangleq \mathbf{x} \setminus \mathbf{a}$. For given optimal solutions $\tilde{\mathbf{x}}$ to problems (33), the *long-term master problem* is expressed as:

$$\min_{\mathbf{a}} \hat{g}(\mathbf{a}) \triangleq \mathbb{E}\{T_o(\mathbf{a})\} \quad (34)$$

$$\text{s.t. (30f), (31b), (31c),}$$

where $T_o(\mathbf{a})$ is rewritten as $T_o(\mathbf{a}) = \frac{\mathbf{a}^T \mathbf{S}_d}{\mathbf{a}^T \mathbf{R}_d} + t_d + t_u + \frac{\mathbf{a}^T \tilde{\mathbf{S}}_u}{\mathbf{a}^T \tilde{\mathbf{R}}_u}$, $\mathbf{S}_d \in \mathbb{R}^N$ is a vector whose elements are S_d , $\tilde{\mathbf{S}}_u \in \mathbb{R}^N$ is a vector whose k -th element is $b_k S_u$, and $\tilde{\mathbf{R}}_u \in \mathbb{R}^N$ is a vector whose k -th element is $b_k R_{u,k}$.

A. Solving the Short-term Subproblem (33)

Problem (33) can be rewritten as

$$\min_{\hat{\mathbf{x}}} \frac{\sum_{k \in \mathcal{N}} a_k S_d}{\sum_{k \in \mathcal{N}} a_k R_{d,k}} + t_d + t_u + \frac{\sum_{k \in \mathcal{N}} a_k b_k S_u}{\sum_{k \in \mathcal{N}} a_k b_k R_{u,k}} \quad (35a)$$

s.t. (14), (24), (30b) – (30e), (32b), (32c),

$$\sigma_{mk}^2 \eta_{mk} \leq \tilde{v}_{mk}, \forall m, k \quad (35b)$$

$$\tilde{v}_{mk} \leq a_k, \forall m, k \quad (35c)$$

$$\sum_{k \in \mathcal{N}} \tilde{v}_{mk} \leq 1, \forall m \quad (35d)$$

$$\zeta_k \leq a_k b_k, \forall k, \quad (35e)$$

where $\hat{\mathbf{x}} \triangleq \{\tilde{\mathbf{x}}, \tilde{\mathbf{v}}\}$ and $\tilde{\mathbf{v}} \triangleq \{\tilde{v}_{mk}\}_{m \in \mathcal{M}, k \in \mathcal{N}}$ are additional variables. Here, (35b)-(35d) follow from (11) and (12); (35e) follows from (18) and (19). If we let $\mathbf{v} \triangleq \{v_{mk}\}_{m \in \mathcal{M}, k \in \mathcal{N}}$ and $\mathbf{u} \triangleq \{u_k\}_{k \in \mathcal{N}}$ with

$$v_{mk} \triangleq \eta_{mk}^{1/2}, \forall m, k, \quad (36)$$

$$u_k \triangleq \zeta_k^{1/2}, \forall k, \quad (37)$$

then (35) can be rewritten as:

$$\min_{\bar{\mathbf{x}}} \frac{\sum_{k \in \mathcal{N}} a_k S_d}{\sum_{k \in \mathcal{N}} a_k R_d} + t_d + t_u + \frac{\sum_{k \in \mathcal{N}} a_k b_k S_u}{\sum_{k \in \mathcal{N}} a_k b_k R_{u,k}} \quad (38a)$$

s.t. (32b), (32c), (35c), (35d)

$$\sigma_{mk}^2 v_{mk}^2 \leq \tilde{v}_{mk}, \forall m, k \quad (38b)$$

$$0 \leq v_{mk}, \forall m, k \quad (38c)$$

$$u_k^2 \leq a_k b_k, \forall m, k \quad (38d)$$

$$0 \leq u_k \leq 1, \forall k \quad (38e)$$

$$0 \leq R_{d,k} \leq h_{d,k}(\mathbf{v}), \forall k \quad (38f)$$

$$0 \leq R_{u,k} \leq h_{u,k}(\mathbf{u}), \forall k. \quad (38g)$$

where $\bar{\mathbf{x}} \triangleq \{\hat{\mathbf{x}}, \mathbf{v}, \mathbf{u}\} \setminus \{\eta, \zeta\}$.

Problem (38) is still challenging due to the nonconvex constraints (38f) and (38g). To deal with these constraints, we note that a function $f(x, y) = \log\left(1 + \frac{|x|^2}{y}\right)$ has the following lower bound [24], [25]:

$$f(x, y) \geq \log \left(1 + \frac{|x^{(\kappa)}|^2}{y^{(n)}} \right) - \frac{|x^{(\kappa)}|^2}{y^{(\kappa)}} + 2 \frac{x^{(n)}x}{y^{(\kappa)}} - \frac{|x^{(\kappa)}|^2(|x|^2 + y)}{y^{(\kappa)}(|x^{(\kappa)}|^2 + y^{(\kappa)})}, \quad (39)$$

where $x \in \mathbb{R}, y > 0, y^{(\kappa)} > 0$. Therefore, the concave lower bound $\tilde{h}_{d,k}(\mathbf{v})$ of $h_{d,k}(\mathbf{v})$ in (38f) is given by

$$\tilde{h}_{d,k}(\mathbf{v}) \triangleq \log_2 \left(1 + \frac{(\Upsilon_k^{(\kappa)})^2}{\Pi_k^{(\kappa)}} \right) - \frac{(\Upsilon_k^{(\kappa)})^2}{\Pi_k^{(\kappa)}} + 2 \frac{\Upsilon_k^{(\kappa)}\Upsilon_k}{\Pi_k^{(\kappa)}} - \frac{(\Upsilon_k^{(\kappa)})^2(\Upsilon_k^2 + \Pi_k)}{\Pi_k^{(\kappa)}((\Upsilon_k^{(\kappa)})^2 + \Pi_k^{(\kappa)})} \leq h_{d,k}(\mathbf{v}), \quad (40)$$

where

$$\begin{aligned} \Upsilon_k(\{v_{mk}\}_{m \in \mathcal{M}}) &= \sqrt{\rho_d} \sum_{m \in \mathcal{M}} v_{mk} \sigma_{mk}^2, \\ \Pi_k(\mathbf{v}) &= \rho_d \sum_{\ell \in \mathcal{N} \setminus k} \left(\sum_{m \in \mathcal{M}} v_{m\ell} \sigma_{m\ell}^2 \frac{\beta_{mk}}{\beta_{m\ell}} \right)^2 |\boldsymbol{\varphi}_\ell^H \boldsymbol{\varphi}_k|^2 + \rho_d \sum_{\ell \in \mathcal{N}} \sum_{m \in \mathcal{M}} v_{m\ell}^2 \sigma_{m\ell}^2 \beta_{mk} + 1. \end{aligned}$$

Similarly, the concave lower bound $\tilde{h}_{u,k}(\mathbf{u})$ of $h_{u,k}(\mathbf{u})$ in (38g) is given by

$$\tilde{h}_{u,k}(\mathbf{u}) \triangleq \log_2 \left(1 + \frac{(\Psi_k^{(\kappa)})^2}{\Xi_k^{(\kappa)}} \right) - \frac{(\Psi_k^{(\kappa)})^2}{\Xi_k^{(\kappa)}} + 2 \frac{\Psi_k^{(\kappa)}\Psi_k}{\Xi_k^{(\kappa)}} - \frac{(\Psi_k^{(\kappa)})^2(\Psi_k^2 + \Xi_k)}{\Xi_k^{(\kappa)}((\Psi_k^{(\kappa)})^2 + \Xi_k^{(\kappa)})} \leq h_{u,k}(\mathbf{u}), \quad (41)$$

where

$$\begin{aligned} \Psi_k(u_k) &= \rho_u^{1/2} u_k \left(\sum_{m \in \mathcal{M}} \sigma_{mk}^2 \right), \\ \Xi_k(\mathbf{u}) &= \rho_u \sum_{\ell \in \mathcal{N} \setminus k} u_\ell^2 \left(\sum_{m \in \mathcal{M}} \sigma_{m\ell}^2 \frac{\beta_{mk}}{\beta_{m\ell}} \right)^2 |\boldsymbol{\varphi}_\ell^H \boldsymbol{\varphi}_k|^2 + \rho_u \sum_{\ell \in \mathcal{N}} u_\ell^2 \sum_{m \in \mathcal{M}} \sigma_{mk}^2 \beta_{m\ell} + \sum_{m \in \mathcal{M}} \sigma_{mk}^2. \end{aligned}$$

As such, (38f) and (38g) can be approximated by

$$R_{d,k} \leq \tilde{h}_{d,k}(\mathbf{v}), \forall k \in \mathcal{N} \quad (42)$$

$$R_{u,k} \leq \tilde{h}_{u,k}(\mathbf{u}), \forall k \in \mathcal{N}. \quad (43)$$

At the iteration $\kappa + 1$, for a given point $\bar{\mathbf{x}}^{(\kappa)}$, problem (38) (hence (33)) can finally be approximated by the following convex problem:

$$\min_{\bar{\mathbf{x}} \in \tilde{\mathcal{F}}} \frac{\sum_{k \in \mathcal{N}} a_k S_d}{\sum_{k \in \mathcal{N}} a_k R_d} + t_d + t_u + \frac{\sum_{k \in \mathcal{N}} a_k b_k S_u}{\sum_{k \in \mathcal{N}} a_k b_k R_{u,k}} \quad (44)$$

where $\tilde{\mathcal{F}} \triangleq \{(32b), (32c), (35c), (35d), (38b) - (38e), (42), (43)\}$ is a convex feasible set.

Algorithm 2 Solving the short-term subproblem (33)

- 1: **Initialization:** Set $\kappa = 1$ and choose a random point $\tilde{\mathbf{x}}^{(0)} \in \mathcal{F}$.
- 2: **repeat**
- 3: Update $\kappa = \kappa + 1$
- 4: Solving (44) to get its optimal solution $\tilde{\mathbf{x}}^*$
- 5: Update $\tilde{\mathbf{x}}^{(\kappa)} = \tilde{\mathbf{x}}^*$
- 6: **until** convergence

Output: $(\boldsymbol{\eta}^*, \boldsymbol{\zeta}^*, \mathbf{f}^*, \mathbf{R}_d^*, \mathbf{R}_u^*)$

In Algorithm 2, we outline the main steps to solve problem (33). Let $\mathcal{F} \triangleq \{(32b), (32c), (35c), (35d), (38b)–(38g)\}$ be the feasible set of (38). Starting from a random point $\bar{\mathbf{x}} \in \mathcal{F}$, we solve (44) to obtain its optimal solution $\bar{\mathbf{x}}^*$. This solution is then used as an initial point in the next iteration. The algorithm terminates when an accuracy level of ε is reached.

Proposition 1. Algorithm 2 converges to a Karush-Kuhn-Tucker (KKT) solution of (33).

Proof. It is true that $\tilde{h}_{d,k}(\mathbf{v})$ and $\tilde{h}_{u,k}(\mathbf{u})$ satisfy the key properties of general inner approximation functions [26, Properties (i), (ii), and (iii)]. The feasible set $\tilde{\mathcal{F}}$ also satisfies the Slater's constraint qualification condition for convex programs. Therefore, Algorithm 2 converges to a KKT solution of (38) when starting from a point $\tilde{\mathbf{x}}^{(0)} \in \mathcal{F}$ [26, Theorem 1]. By using the variable transformations (36) and (37), it can be seen that the KKT solutions of (38) satisfy the KKT conditions of (35) as well as of (33). \square

B. Solving the Long-Term Master Problem (34)

Given solution $\tilde{\mathbf{x}}$ to short-term subproblems (33), we have $t_d = \frac{a_{k^*} S_d}{R_{d,k^*}}$, where $k^* \triangleq \operatorname{argmax}_{k \in \mathcal{N}} \frac{a_k S_d}{R_{d,k}}$. Therefore, we can have $t_d = \mathbf{a}^T \tilde{\mathbf{t}}_d$, where $\tilde{\mathbf{t}}_d$ is the vector whose elements are 0 except for the k^* -th element, and the value of this element is $\frac{S_d}{R_{d,k^*}}$. Similarly, $t_u = \frac{a_{j^*} b_{j^*} S_u}{R_{u,j^*}}$ with $j^* \triangleq \operatorname{argmax}_{k \in \mathcal{N}} \frac{a_k b_k S_u}{R_{u,k}}$ and $b_{j^*} = 1$. It can be rewritten as $t_u = \mathbf{a}^T \tilde{\mathbf{t}}_u$, where $\tilde{\mathbf{t}}_u$ is the vector whose elements are 0 except for the j^* -th element, and the value of this element is $\frac{S_u}{R_{u,j^*}}$. Now, the long-term problem (34) is equivalent to

$$\begin{aligned} \min_{\mathbf{a}} g(\mathbf{a}) &\triangleq \mathbb{E} \left\{ \frac{\mathbf{a}^T \mathbf{S}_d}{\mathbf{a}^T \mathbf{R}_d} + \mathbf{a}^T \tilde{\mathbf{t}}_d + \mathbf{a}^T \tilde{\mathbf{t}}_u + \frac{\mathbf{a}^T \tilde{\mathbf{S}}_u}{\mathbf{a}^T \tilde{\mathbf{R}}_u} \right\} \\ &\text{s.t. (30f), (31b), (31c).} \end{aligned} \quad (45)$$

Let $V(\mathbf{a}) \triangleq \sum_{k \in \mathcal{N}} (a_k - a_k^2) = \mathbf{a}^T (\mathbf{1} - \mathbf{a})$, then (31b) becomes $V(\mathbf{a}) \leq 0$. We now consider the problem

$$\begin{aligned} \min_{\mathbf{a}} \quad & \mathcal{L}(\mathbf{a}, \lambda) \triangleq g(\mathbf{a}) + \lambda V(\mathbf{a}) \\ \text{s.t.} \quad & (30\text{f}), (31\text{c}), \end{aligned} \quad (46)$$

where $\mathcal{L}(\mathbf{a}, \lambda)$ is the Lagrangian of (45), λ is the Lagrangian multiplier corresponding to (31b), and $\mathbf{1} \in \mathbb{R}^N$ is an all-one vector. Let $\mathcal{H} \triangleq \{(30\text{f}), (31\text{c})\}$ be the feasible set of the problem (34).

Proposition 2. The following statement holds:

- (i) The value of V_λ at the solution of (34) corresponding to λ is decreasing to 0 as $\lambda \rightarrow +\infty$.
- (ii) Problem (46) has the following property, i.e.,

$$\min_{\mathbf{a} \in \mathcal{H}} g(\mathbf{a}) = \sup_{\lambda \geq 0} \min_{\mathbf{a} \in \mathcal{H}} \mathcal{L}(\mathbf{a}, \lambda) \quad (47)$$

and is therefore equivalent to (45) at the optimal solution $\lambda^* \geq 0$ of the sup-min problem in (47).

Proof. The proof is rather standard, and follows from [22, Proposition 1], [21, Proposition 1]. \square

Theoretically, it is required to have $V_\lambda = 0$ in order to obtain an optimal λ^* . According to Proposition 1, V_λ decreases to 0 as $\lambda \rightarrow +\infty$. Since there is always a numerical tolerance in computation, it is sufficient to accept $V_\lambda < \varepsilon$ for some small ε with a sufficiently large value of λ chosen. In our numerical experiment, for $\varepsilon = 0.001$, we see that $\lambda = 1$ is enough to ensure $V_\lambda \leq \varepsilon$. Note that this way of choosing λ has been widely used in the literature, e.g., [21], [22], [27], [28].

At the large-scale coherence time or iteration $n + 1$, problem (34) is approximated by the following convex problem:

$$\min_{\mathbf{a} \in \mathcal{H}} \bar{\mathcal{L}}(\mathbf{a}), \quad (48)$$

where $\bar{\mathcal{L}}(\mathbf{a})$ is a surrogate function of $\mathcal{L}(\mathbf{a})$, and it is defined as

$$\begin{aligned} \bar{\mathcal{L}}(\mathbf{a}) \triangleq & \mathcal{L}^{(n+1)} + ((\nabla \mathcal{L})^{(n+1)})^T (\mathbf{a} - \mathbf{a}^{(n+1)}) \\ & + \tau \|\mathbf{a} - \mathbf{a}^{(n+1)}\|^2; \\ \mathcal{L}^{(n+1)} = & \bar{g}^{(n+1)} + \lambda V^{(n+1)} \end{aligned} \quad (49)$$

$$\begin{aligned}
\bar{g}^{(n+1)} &= (1 - \phi^{(n+1)})\bar{g}^{(n)} + \phi^{(n+1)}T^{(n+1)} \\
(\nabla \mathcal{L})^{(n+1)} &= (\nabla \bar{g})^{(n+1)} + \lambda(\nabla V)^{(n+1)} \\
(\nabla \bar{g})^{(n+1)} &= (1 - \phi^{(n+1)})\nabla \bar{g}^{(n)} + \phi^{(n+1)}\nabla T^{(n+1)}.
\end{aligned}$$

Here, $\bar{g}^{(0)} = 0$, $(\nabla \bar{g})^{(0)} = \mathbf{0}$, $\phi^{(n+1)}$ is a weighting parameter,

$$(\nabla T)^{(n+1)} = \frac{\mathbf{S}_d((\mathbf{a}^{(n+1)})^T \mathbf{R}_d) - \mathbf{R}_d((\mathbf{a}^{(n+1)})^T \mathbf{S}_d)}{((\mathbf{a}^{(n+1)})^T \mathbf{R}_d)^2} + \frac{\tilde{\mathbf{S}}_u((\mathbf{a}^{(n+1)})^T \tilde{\mathbf{R}}_u) - \tilde{\mathbf{R}}_d((\mathbf{a}^{(n+1)})^T \tilde{\mathbf{S}}_u)}{((\mathbf{a}^{(n+1)})^T \tilde{\mathbf{R}}_u)^2} + \tilde{\mathbf{t}}_d + \tilde{\mathbf{t}}_u,$$

and $(\nabla V)^{(n+1)} = \mathbf{1} - 2\mathbf{a}^{(n+1)}$.

C. Solving the Overall Problem (30)

Algorithm 3 outlines the main steps to solve the overall problem (30). In the large-scale coherence time n , for a given random value of $\mathbf{a}^{(n+1)} \in \mathcal{H}$, the set $\tilde{\mathcal{N}}^{(n+1)}$ of the selected UEs is constructed by (3). The index set $\mathcal{S}^{(n+1)}$ of sampled UEs in $\tilde{\mathcal{N}}^{(n+1)}$ is chosen by (17). The short-term subproblem (33) is solved by Algorithm 2 after $I_S^{(n)}$ iterations to obtain a KKT solution. This solution is then used to construct the approximate long-term master problem (46). After solving (46) to obtain an optimal solution $(\mathbf{a}^*)^{(n+1)}$, we update $\mathbf{a}^{(n+2)}$ as

$$a_k^{(n+2)} = (1 - \pi^{(n+1)})a_k^{(n+1)} + \pi^{(n+1)}(a_k^*)^{(n+1)}, \forall k \quad (50)$$

where $\pi^{(n+1)}$ is a weighting parameter; $\{\phi^{(n)}, \pi^{(n)}\}$ is chosen to satisfy the following conditions [18, Assumption 5].

(A1): $\phi^{(n)} \rightarrow 0$, $\frac{1}{\phi^{(n)}} \leq \mathcal{O}(n^\zeta)$ for $\zeta \in (0, 1)$, and $\sum_n (\phi^{(n)})^2 < \infty$;

(A2): $\pi^{(n)} \rightarrow 0$, $\sum_n \pi^{(n)} = \infty$, $\sum_n (\pi^{(n)})^2 < \infty$, and $\lim_{n \rightarrow \infty} \frac{\pi^{(n)}}{\phi^{(n)}} = 0$.

The REPEAT-UNTIL loop continues until Algorithm 3 converges.

D. The Proposed Algorithm: Convergence Analysis

Once Algorithm 3 converges, the FL process is then executed using the solution \mathbf{a} obtained by Algorithm 3. Here, the transmission performance of training update in each iteration of the FL process is enhanced by updating $(\boldsymbol{\eta}, \boldsymbol{\zeta}, \mathbf{R}_d, \mathbf{R}_u)$ using Algorithm 2 in each large-scale coherence time. Before starting any new FL process, Algorithm 3 is executed again.

Algorithm 3 UE selection to Mitigate Straggler Effect for FL on CFmMIMO networks

- 1: **Initialization:** Set $n = 0$, select a random $\mathbf{a}^{(n+1)} \in \mathcal{H}$
- 2: **repeat**
- 3: Update $\tilde{\mathcal{N}}^{(n+1)}$ by (3), and choose $\mathcal{S}^{(n+1)}$ from $\tilde{\mathcal{N}}$ by (17)
- 4: Solve the short-term subproblem (33) to obtain its optimal solution $(\boldsymbol{\eta}^*, \boldsymbol{\zeta}^*, \mathbf{R}_d^*, \mathbf{R}_u^*)$ by using Algorithm 2, and update $(\boldsymbol{\eta}^{(n+1)}, \boldsymbol{\zeta}^{(n+1)}, \mathbf{R}_d^{(n+1)}, \mathbf{R}_u^{(n+1)}) = (\boldsymbol{\eta}^*, \boldsymbol{\zeta}^*, \mathbf{R}_d^*, \mathbf{R}_u^*)$
- 5: Solve the approximate long-term master problem (48) to obtain its optimal solution $(\mathbf{a}^*)^{(n+1)}$
- 6: Update $\mathbf{a}^{(n+2)}$ by (50)
- 7: Update $n = n + 1$
- 8: **until** convergence

Output: $\mathbf{a}^* = \mathbf{a}^{(n+1)}$

Definition 1. A solution $(\mathbf{a}^*, \mathbf{x}^*)$ is called a stationary solution of problem (31) or the main problem (30) if \mathbf{x}^* is a KKT solution of the short-term subproblem (33) for $\mathbf{a} = \mathbf{a}^*$, and \mathbf{a}^* is a KKT solution of the long-term master problem (34) for $\mathbf{x} = \mathbf{x}^*$.

Proposition 3. Algorithm 3 converges to the neighbourhood of the stationary solutions to problem (30).

Proof. See Appendix A. □

Theoretically, $I_S^{(n)} \rightarrow \infty$ and $\lambda \rightarrow \infty$ are required for Algorithm 3 to converge to the stationary solutions to problem (30). When $I_S^{(n)}$ and λ are finite, Algorithm 3 converges to approximate stationary solutions of problem (30).

V. SUBOPTIMAL APPROACH

The previous section proposes an “optimal” approach to achieve the lowest transmission time of one iteration of an FL process by the joint optimization of Steps (S1) and (S3). In this section, we introduce a suboptimal approach to reduce the transmission time.

We first observe that the straggler effect is more serious in Step (S1) than that in Step (S3). As can be seen from (26) and (27), this effect always happens in Step (S1) due to the UEs with unfavorable links while in Step (S3), it happens only when the UEs with unfavorable links are sampled. Therefore, the suboptimal scheme selects $\tilde{N} \geq K$ UEs out of the original N UEs to achieve the lowest transmission time of only Step (S1). The obtained solution \mathbf{a} is then used for both Steps (S1) and (S2) during the FL process.

Since we focus only on Step (S1), the transmission time minimization problem is a simplified version of problem (30) as

$$\begin{aligned} \min_{\mathbf{a}, \eta, \mathbf{R}_d} \hat{g}(\mathbf{a}, \mathbf{R}_d) &\triangleq \mathbb{E}\{T_d(\mathbf{a}, \mathbf{R}_d)\} \\ \text{s.t. } &(1), (11), (12), (14), (30b), (30d), (30f). \end{aligned} \quad (51a)$$

Since the mathematical structure of (51) is the same as that of (30), the proposed Algorithm 3 can be used to solve (51) with a slight modification. Given the UE selection solutions obtained from solving (51), the mathematical structure of the problem that optimizes power and rates to minimize the transmission time of Step (S1) is also the same as that of the short-term subproblem (33). Therefore, it is solved by Algorithm 2.

It should be noted that since problem (51) does not have the variables of UL power control and UL data rate for Step (S3), problem (51) is less complex than problem (30). Therefore, it is expected that the complexity of the algorithm to solve the problem (51) in the suboptimal method is less than that to solve the problem (30) in the optimal approach.

Remark 3. Our optimal and suboptimal approaches select UEs before any FL process is executed, and hence, they do not affect the FL processes during their executing time. They also have no requirement on the ML models. These properties make our approaches different from the existing UE selection methods which select UEs in each iteration of one FL process [12], [14]. The methods in [12], [14] require a joint design of UE selection and the FL framework to make sure the FL process converges. Moreover, the convergence of the FL process using such methods also requires some strict conditions of the ML models such as [12, Assumptions 2, 3].

VI. NUMERICAL EXAMPLES

A. Network Setup with Non-Uniform UE/AP Distribution

We consider a CFmMIMO network in a square Q of $D \times D$ km² whose edges are wrapped around to avoid the boundary effects. To better analyze the effectiveness of the proposed UE selection approaches, the locations of APs and UEs are generated by using two models for two practical cases as follows. The first case (C1) is described by three properties:

- (P1): The UEs are more likely to stay close to some local points.
- (P2): Some local areas attract more UEs than other local areas.
- (P3): The APs are uniformly located in the network.

The second case (C2) is the case (C1) with the property (P3) replaced by two more practical properties:

(P4): The APs are more likely to locate close to some local points.

(P5): Some local areas have more APs than other local areas.

1) *Modelling case (C1)*: We recall that in a cellular network, [29] proposes a method to let the UEs stay close to the base stations. Here, we adopt this method to model the property (P1). First, let Φ be a homogeneous Poisson Point Process (PPP) in Q with a density μ , and ϕ be the number of the Poisson Points (PPs) in Φ . Denote by $\mathcal{V} \triangleq \{\mathcal{V}_1, \dots, \mathcal{V}_\phi\}$ the set of all Voronoi cells that are generated from these PPs. Φ is then thinned by retaining points in Φ independently with probability p and removing the rest. The thinned version Φ_p of Φ models the local points that attract UEs and the Voronoi cells corresponding to the PPs of Φ_p models their local areas.

Let \mathcal{I} be the set of indices of the PPs retained in Φ . Here, the UEs are then uniformly distributed in the Voronoi cells of these PPs, i.e., $\{\mathcal{V}_i\}_{i \in \mathcal{I}}$. Since the Voronoi cells of Φ_p is larger than those of the retained points of Φ , the UEs are thus pushed towards the interior of the local areas, which captures the property (P1). Here, the larger thinning probability p implies the higher probability of a UE in a Voronoi cell close to its local point.

To capture the property (P2), we set a probability p_i for the local area $i \in \mathcal{I}$ that is chosen to come by each UE. We assume that $\{p_i\}_{i \in \mathcal{I}}$ are the same for all the UEs. In each realization, we randomly choose a set $\{p_i\}_{i \in \mathcal{I}}$ such that $\sum_{i \in \mathcal{I}} p_i = 1$ and $\max_i p_i - \min_i p_i = \Delta$, where Δ controls the difference in the attraction of the local areas. Each UE $k \in \mathcal{N}$ is then selected to the local area i with probabilities $\{p_i\}_{i \in \mathcal{I}}$. Finally, the selected UEs in each local area $i \in \mathcal{I}$ is uniformly distributed in the corresponding Voronoi cells \mathcal{V}_i .

2) *Modelling case (C2)*: To capture the properties (P4) and (P5), the APs are non-uniformly distributed using the same method that captures the properties (P1) and (P2).

3) *Setup for each network realization*: In each network realization, the locations of APs are fixed and those of the UEs change over the iterations of the FL process. Since each iteration of the FL process happens in one large-scale coherence time (in the order of seconds), the total running time of an FL process is expected to be around several minutes. Therefore, we assume that the UEs only move around their current local areas during the FL process. Here, in each iteration of the FL process of each network setup realization, the locations of UEs are uniformly distributed in the Voronoi cells that those UEs belong to.

B. Parameters Setting

We set $\tau_c = 200$ samples. The large-scale fading coefficients, e.g., β_{mk} , are modeled in the same manner as [30]

$$\beta_{mk} = 10^{\frac{\text{PL}_{mk}^d}{10}} 10^{\frac{F_{mk}}{10}}, \quad (52)$$

where $10^{\frac{F_{mk}}{10}}$ represents the shadowing effect with $F_{mk} \in \mathcal{N}(0, 4^2)$ (in dB); and $10^{\frac{\text{PL}_{mk}^d}{10}}$ represents the path loss. Here, PL_{mk}^d (in dB) is given by

$$\text{PL}_{mk}^d = -30.5 - 36.7 \log_{10} \left(\frac{d_{mk}}{1 \text{ m}} \right) \quad (53)$$

and the correlation among the shadowing term from the AP $m, \forall m \in \mathcal{M}$ to different UEs $k, \ell \in \mathcal{N}$ is expressed as

$$\mathbb{E}\{F_{mk}F_{j\ell}\} \triangleq \begin{cases} 4^2 2^{-\delta_{k\ell}/9\text{m}}, & \text{if } j = m \\ 0, & \text{otherwise,} \end{cases}, \forall j \in \mathcal{M}, \quad (54)$$

where $\delta_{k\ell}$ is the distance between UEs k and ℓ . To estimate channels, a random pilot assignment is used. Specifically, the pilot of each user is randomly chosen from a predefined set of τ_t orthogonal pilot sequences, each of length τ_t samples.

Here, we choose a thinning probability $p = 0.3$, $\Delta = 1/4$ for UEs and $\Delta = 1/10$ for APs, $\tau_t = 10$, $S_d = S_u = 0.5$ MB, and noise power $\sigma_0^2 = -92$ dBm. Let $\tilde{\rho}_d = 1$ W, $\tilde{\rho}_u = 0.2$ W and $\tilde{\rho}_t = 0.2$ W be the maximum transmit power of the APs, UEs and UL pilot sequences, respectively. The maximum transmit powers ρ_d , ρ_u and ρ_t are normalized by the noise power. We set $\pi^{(n)} = \frac{100}{100+n}$ and $\phi^{(n)} = \frac{1}{n^{9/10}}$ which satisfy conditions (A1) and (A2) in Section IV-C.

C. Results and Discussions

1) *Effectiveness of the proposed algorithms:* First, we evaluate the convergence behavior of the proposed Algorithm 3. As seen from Fig. 2 with an arbitrary network realization, Algorithm 3 converges in around 30 iterations. It is also worth noting that each iteration of Algorithm 3 corresponds to solving simple convex programs (44) and (48). It is therefore expected that Algorithm 3 has a low computational complexity.

To further evaluate the effectiveness of Algorithm 3, we consider the following baseline schemes:

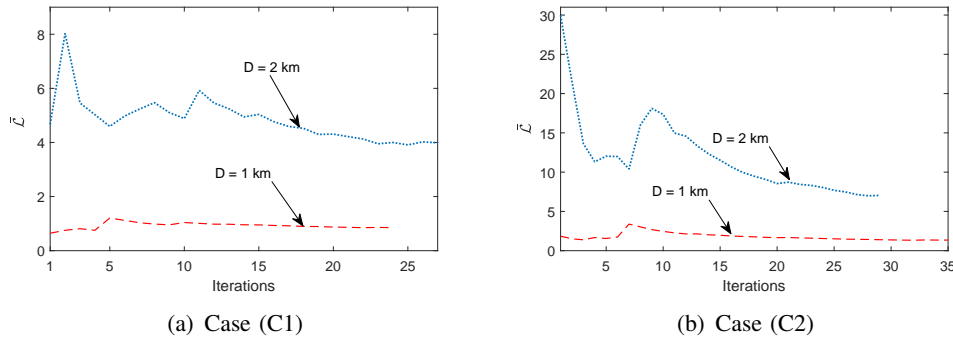


Fig. 2. The convergence of Algorithm 3. Here, $M = 10$, $N = 6$, $N_{\text{QoL}} = 3$, $K = 3$.

- Baseline 1 (BL1): UE selection is not optimized. The transmitted powers and rates of Steps (S1) and (S3) for all N original UEs are optimized by using a slightly modified version of Algorithm 2.
- Baseline 2 (BL2): This baseline is similar to BL1 except that the UEs are selected by randomly choosing \hat{N} UEs from the original N UEs, where $\hat{N} \in [N_{\text{QoL}}, N-1]$ is a random number.

Here, in each network realization, the effective transmission times T_e of one iteration of an FL process in baselines (BL1) and (BL2) are the average times over the large-scale fading realizations. For ease of presentation, our “optimal” UE selection approach is denoted by “OPT” and our suboptimal approach is denoted by “SUB”.

Fig. 3 shows the comparison among the considered schemes in terms of the effective transmission time T_e of each iteration of an FL process. As seen, OPT gives the best performance while SUB achieves the performance close to that of OPT. In particular, while BL1 and BL2 achieve nearly the same performance, OPT provides substantial time reductions over these schemes, e.g., up to 52% in case (C1) and 63% in case (C2) with $M = 10$ and $D = 2$ km. OPT only provides a marginal time reduction over SUB, i.e., up to 15% in both cases.

The figure also shows the importance of UE selection in reducing the FL training time, especially with the practical case (C2) in the networks that have a moderately low density of APs, i.e., having a large value of D and a small/moderate number of APs. This is because the straggler effect becomes serious in such these cases. In particular, compared to the transmission time T_e obtained by BL1, the amount of time reduction by OPT with case (C2), $M = 10$ and $D = 2$ km is 20% larger than that with case (C1), and approximately twice that with $D = 1$ km. The amount of time reduction by OPT also increases when the number of APs decreases.

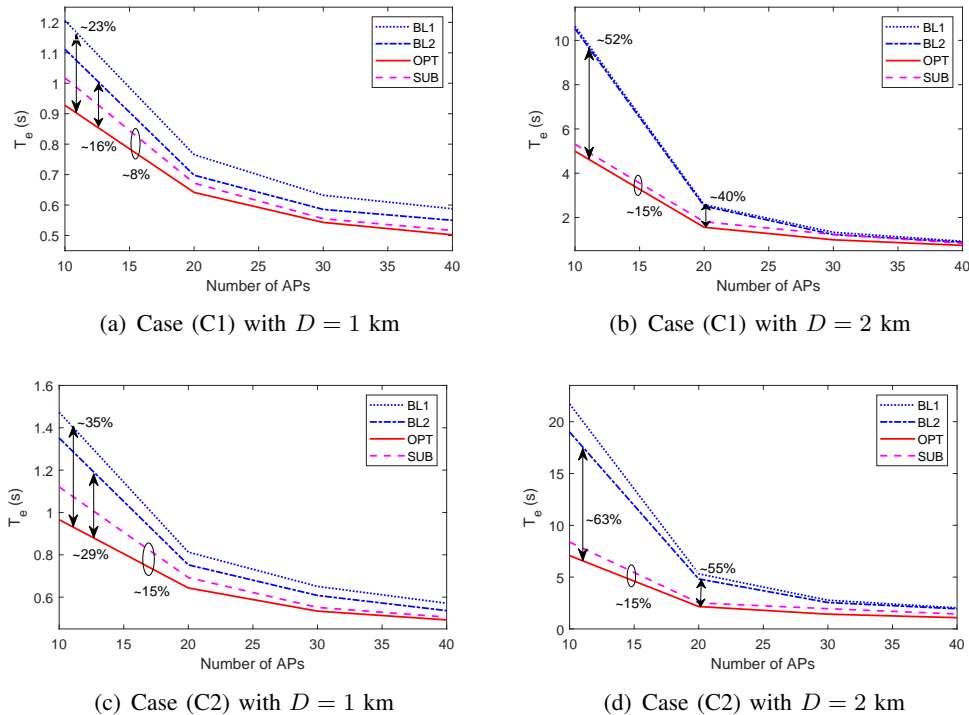


Fig. 3. The effectiveness of the proposed approaches. Here, $N = 6$, $N_{QoL} = 3$ and $K = 3$.

These facts are reasonable because in case (C2), the APs are located close to some local points which may be far from the UE locations. This makes the probability of UEs with unfavorable links higher than that in case (C1) where the AP locations are uniformly distributed over the whole area. When D is large, there are more UEs that have unfavorable links for a larger area. Moreover, due to the smaller array gain, the data rates of UEs decrease when the number of APs decreases.

2) *Impact of the number sampled UEs K on the transmission time of one iteration of an FL process:* The impact of the number K of sampled UEs on the effective transmission time T_e of one iteration of an FL process is shown Fig. 4. Here, decreasing K leads to a reduction in T_e . Specifically, this reduction is up to 58% in case (C2) with $K = 2, D = 2$ km compared to that with $K = 5$. This is reasonable because at a lower value of K , UE sampling has more contribution to the reduction of the transmission time of Step (S3). It can also be seen from Fig. 4 that the impact of K on T_e in case (C2) with a large value of D is stronger than those in other cases. This is because the straggler effect is more serious in these cases as discussed in Section VI-C-1).

3) *Impact of N_{QoL} on the transmission time of one iteration of an FL process:* Fig. 5 shows the impact of N_{QoL} on the transmission time of one iteration of an FL process. As seen, increasing

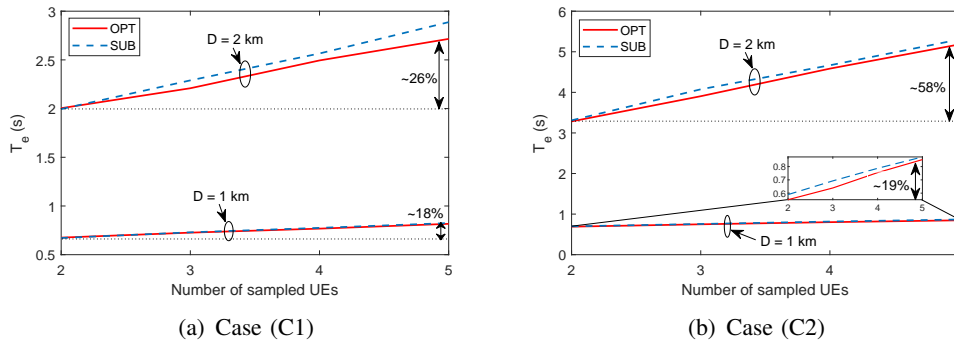


Fig. 4. Impact of the number K of sampled UEs. Here, $M = 20$, $N = 6$, and $N_{\text{QoL}} = 5$.

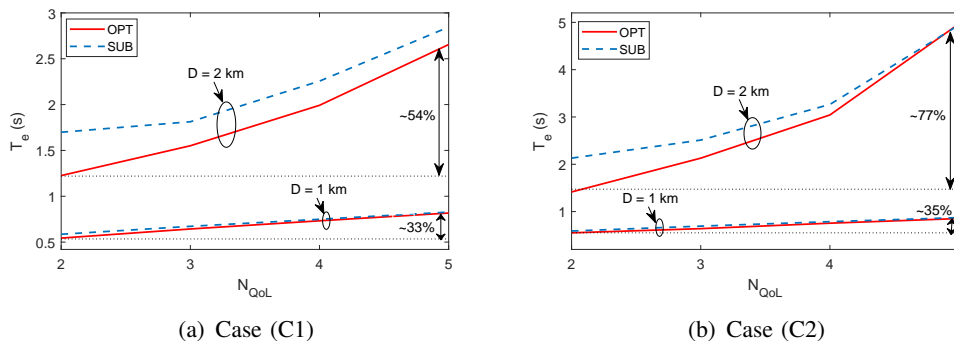


Fig. 5. Impact of the threshold N_{QoL} to ensure the quality of leaning. Here, $M = 20$, $N = 6$, and $K = N_{\text{QoL}}$.

N_{QoL} leads to a dramatic increase in the effective transmission time T_e , e.g., by up to 77% with $D = 2$, $N_{\text{QoL}} = 5$ in comparison to that with $N_{\text{QoL}} = 2$. This is because at a larger value of N_{QoL} , more UEs are required to participate in an FL process. The mutual interference and pilot contamination become stronger for a larger number of UEs. This leads to an increase in the time required to complete the transmission of training updates in one iteration of the FL process.

VII. CONCLUSION

In this work, we have proposed two UE selection approaches to mitigate the straggler effect for FL on CFmMIMO networks. Targeting the training time minimization for the general FL framework with UE sampling [10], [11], we have jointly designed UE selection, power control, and data rate under practical requirements on the maximum transmit powers of APs and UEs, and the minimum number of UEs to guarantee the quality of learning. Two mixed-integer mixed-timescale stochastic nonconvex problems were formulated for these two approaches with the objectives of minimizing the training time of one FL process. Utilizing the general online successive convex approximation framework for solving only mixed-timescale stochastic nonconvex problems, we have successfully developed a novel algorithm to solve the formulated problems.

The proposed algorithm has been proved to converge to the neighbourhood of stationary points. Numerical results have showed that our UE selection designs significantly reduce the FL training time over the baselines under comparison, especially in a network that a moderately low density of APs. They have also confirmed that the number of sampled UEs and the minimum number of UEs to guarantee the quality of learning have remarkable impacts on the FL training time.

APPENDIX A

PROOF OF PROPOSITION 3

Proposition 3 can be proved using two steps. The first step is to prove the solution \mathbf{x}^* obtained from Algorithm 3 is a KKT solution of the short-term subproblem (33). The second step is to prove the solution $\mathbf{a}^{(n+1)}$ obtained from Algorithm 3 is a KKT solution of the long-term master problem (34). While the first step is completed from Proposition 1, the second step is stated in the following.

It can be confirmed that the problem (30) satisfies the conditions of the Assumption 1 on the main problem in the general framework [18]. It is worth noting that we do not verify Assumption 1-5) and Assumption 1-6) in [18] because of the following reasons. Assumption 1-5) on Mangasarian-Fromovitz constraint qualification is used to ensure the existence of KKT solutions of the short-term subproblem (33). In this work, since Proposition 1 shows that a KKT solution of (33) can be obtained by Algorithm 2, this assumption is unnecessary. Assumption 1-6) is used to guarantee a convergence to an exact stationary point of the short-term subproblem (33). However, [18] confirms that Assumption 1-6) can be removed when we allow an approximate convergence by solving the short-term subproblem (33) with a finite number of iterations.

From the definitions of $\tilde{h}_{d,k}(\mathbf{v})$, and $\tilde{h}_{u,k}(\mathbf{u})$ in (40) and (41), it can be verified that $\tilde{h}_{d,k}(\mathbf{v})$ and $\tilde{h}_{u,k}(\mathbf{u})$ have the following properties:

- $\tilde{h}_{d,k}(\mathbf{v}^{(n)}) = h_{d,k}(\mathbf{v}^{(n)})$, $\tilde{h}_{u,k}(\mathbf{u}^{(n)}) = h_{u,k}(\mathbf{u}^{(n)})$, $\nabla \tilde{h}_{d,k}(\mathbf{v}^{(n)}) = \nabla h_{d,k}(\mathbf{v}^{(n)})$, $\nabla \tilde{h}_{u,k}(\mathbf{u}^{(n)}) = \nabla h_{u,k}(\mathbf{u}^{(n)})$;
- $-\tilde{h}_{d,k}(\mathbf{v})$, and $-\tilde{h}_{u,k}(\mathbf{u})$ are strongly convex;
- $\tilde{h}_{d,k}(\mathbf{v}, \mathbf{v}^{(n)})$ and $\tilde{h}_{u,k}(\mathbf{u}, \mathbf{u}^{(n)})$ are Lipschitz continuous in both $\mathbf{v}, \mathbf{v}^{(n)}$ and both $\mathbf{u}, \mathbf{u}^{(n)}$, respectively.

Algorithm 2 thus satisfies all the conditions of Assumption 2 on the short-term algorithm of the general framework [18]. Since $\{\phi^{(n)}, \pi^{(n)}\}$ are chosen to satisfy (A1) and (A2), they satisfy all the conditions of Assumption 5 in [18]. When Assumptions 1, 2 and 5 in [18] is satisfied, it

is confirmed by [18, Corollary 1] that the surrogate function $\bar{g}(\mathbf{a})$ chosen as (49) satisfies the Assumption 3 and 4 in [18] on the properties and asymptotic consistency of surrogate functions.

Since Assumptions 1-5 in [18] are all satisfied, it follows from [18, Lemma 1] that:

- (i) The sequence $\{(\mathbf{a}^{(n+1)}, (\mathbf{a}^*)^{(n+1)})\}_{n=1}^{\infty}$ generated over iterations of Algorithm 3 has the following property.

$$\lim_{n \rightarrow \infty} \|\mathbf{a}^{(n+1)} - (\mathbf{a}^*)^{(n+1)}\| = 0. \quad (55)$$

- (ii) Let \mathbf{a}_* be a limit point of a subsequence $\{\mathbf{a}^{(n+1)_j}\}_{j=1}^{\infty}$ and

$$\lim_{j \rightarrow \infty} |\bar{g}(\mathbf{a}^{(n+1)_j}) - g(\mathbf{a}_*)| = 0, \quad (56)$$

$$\lim_{j \rightarrow \infty} |\nabla \bar{g}(\mathbf{a}^{(n+1)_j}) - \nabla g(\mathbf{a}_*)| = 0. \quad (57)$$

Without loss of generality, we assume that $\mathbf{a}^{(n+1)} \rightarrow \mathbf{a}_*$ as $n \rightarrow \infty$. Then, (56) and (57) imply that

$$\lim_{n \rightarrow \infty} |\bar{g}(\mathbf{a}^{(n+1)}) - g(\mathbf{a}^{(n+1)})| = 0, \quad (58)$$

$$\lim_{n \rightarrow \infty} |\nabla \bar{g}(\mathbf{a}^{(n+1)}) - \nabla g(\mathbf{a}^{(n+1)})| = 0. \quad (59)$$

It can be seen that there always exists one interior point in \mathcal{H} . Therefore, the convex problem (48) satisfies the Slater's constraint qualification condition, and hence, its optimal solution $(\mathbf{a}^*)^{(n+1)}$ is a KKT solution to (46) (hence, to (34)), i.e.,

$$\nabla \bar{g}((\mathbf{a}^*)^{(n+1)}) + \sum_{j=1}^r \nu_j \nabla \delta_j((\mathbf{a}^*)^{(n+1)}) = 0, \quad (60a)$$

$$\nu_j \delta_j((\mathbf{a}^*)^{(n+1)}) = 0, \forall j \in \{1, \dots, q\}, \quad (60b)$$

where $\delta_j(\mathbf{a}), \forall j \in \{1, \dots, q\}$ represent the functions in the constraints (30f), (31b) and (31c). It follows from (55) and (59) that the gap between $\mathbf{a}^{(n+1)}$ and $(\mathbf{a}^*)^{(n+1)}$ and that between $\nabla \bar{g}(\mathbf{a}^{(n+1)})$ and $\nabla g(\mathbf{a}^{(n+1)})$ converge to zero as $n \rightarrow \infty$. Therefore, (60) implies

$$\nabla g(\mathbf{a}^{(n+1)}) + \sum_{j=1}^r \nu_j \nabla \delta_j(\mathbf{a}^{(n+1)}) = 0, \quad (61a)$$

$$\nu_j \delta_j(\mathbf{a}^{(n+1)}) = 0, \forall j \in \{1, \dots, r\}, \quad (61b)$$

which means $\mathbf{a}^{(n+1)}$ is a KKT solution of the long-term master problem (34).

As such, the convergence of Algorithm 3 to a stationary point of problem (30) in the sense of Definition 1 are guaranteed if the numbers of iterations of Algorithms 2 and 3 are infinity, i.e., $I_S^{(n)} \rightarrow \infty$, $I_L \rightarrow \infty$. In practice, it is acceptable to choose finite $\{I_S^{(n)}\}_{n \in \{1, \dots, I_L\}}$ and I_L for an approximate convergence. Therefore, Algorithm 3 is guaranteed to converge to the neighbourhood of the stationary solutions of problem (30).

REFERENCES

- [1] Cisco, “Cisco annual internet report,” Mar. 2020. [Online]. Available: <https://www.cisco.com/c/en/us/solutions/collateral/executive-perspectives/annual-internet-report/white-paper-c11-741490.html>
- [2] J. Dong, M. Noreikis, Y. Xiao, and A. Yl-Jski, “Vinav: A vision-based indoor navigation system for smartphones,” *IEEE Trans. Mobile Comput.*, vol. 18, no. 6, pp. 1461–1475, Jun. 2019.
- [3] K. B. Letaief, W. Chen, Y. Shi, J. Zhang, and Y. A. Zhang, “The roadmap to 6G: AI empowered wireless networks,” *IEEE Commun. Mag.*, vol. 57, no. 8, pp. 84–90, Aug. 2019.
- [4] F. D. Calabrese, L. Wang, E. Ghadimi, G. Peters, L. Hanzo, and P. Soldati, “Learning radio resource management in RANs: Framework, opportunities, and challenges,” *IEEE Commun. Mag.*, vol. 56, no. 9, pp. 138–145, Sep. 2018.
- [5] G. Zhu, D. Liu, Y. Du, C. You, J. Zhang, and K. Huang, “Toward an intelligent edge: Wireless communication meets machine learning,” *IEEE Commun. Mag.*, vol. 58, no. 1, pp. 19–25, 2020.
- [6] S. Niknam, H. S. Dhillon, and J. H. Reed, “Federated learning for wireless communications: Motivation, opportunities, and challenges,” *IEEE Commun. Mag.*, vol. 58, no. 6, pp. 46–51, 2020.
- [7] T. Li, A. K. Sahu, A. Talwalkar, and V. Smith, “Federated learning: Challenges, methods, and future directions,” *IEEE Signal Process. Mag.*, vol. 37, no. 3, pp. 50–60, 2020.
- [8] Z. Du, C. Wu, T. Yoshinaga, K. A. Yau, Y. Ji, and J. Li, “Federated learning for vehicular internet of things: Recent advances and open issues,” *IEEE Open J. Comput. Soc.*, vol. 1, pp. 45–61, 2020.
- [9] B. McMahan, E. Moore, D. Ramage, S. Hampson, and B. A. y Arcas, “Communication-efficient learning of deep networks from decentralized data,” in *Proc. Int. Conf. Artificial Intell. Stat. (AISTATS)*, 2017, pp. 1273–1282.
- [10] X. Li, K. Huang, W. Yang, S. Wang, and Z. Zhang, “On the convergence of FedAvg on Non-IID data,” in *Proc. Int. Conf. Learning Representations (ICLR)*, 2020.
- [11] F. Haddadpour and M. Mahdavi, “On the convergence of local descent methods in federated learning,” 2019. [Online]. Available: <https://arxiv.org/abs/1910.14425>
- [12] W. Xia, T. Q. S. Quek, K. Guo, W. Wen, H. H. Yang, and H. Zhu, “Multi-armed bandit based client scheduling for federated learning,” *IEEE Trans. Wireless Commun.*, 2020.
- [13] W. Shi, S. Zhou, and Z. Niu, “Device scheduling with fast convergence for wireless federated learning,” in *Proc. IEEE Int. Conf. Commun. (ICC)*, 2020, pp. 1–6.
- [14] M. Chen, H. V. Poor, W. Saad, and S. Cui, “Convergence time minimization of federated learning over wireless networks,” in *Proc. IEEE Int. Conf. Commun. (ICC)*, 2020, pp. 1–6.
- [15] T. T. Vu, D. T. Ngo, N. H. Tran, H. Q. Ngo, M. N. Dao, and R. H. Middleton, “Cell-free massive MIMO for wireless federated learning,” *IEEE Trans. Wireless Commun.*, 2020.

- [16] H. Q. Ngo, A. Ashikhmin, H. Yang, E. G. Larsson, and T. L. Marzetta, "Cell-free massive MIMO versus small cells," *IEEE Trans. Wireless Commun.*, vol. 16, no. 3, pp. 1834–1850, Mar. 2017.
- [17] T. L. Marzetta, E. G. Larsson, H. Yang, and H. Q. Ngo, *Fundamentals of Massive MIMO*. Cambridge University Press, 2016.
- [18] A. Liu, V. K. N. Lau, and M. Zhao, "Online successive convex approximation for two-stage stochastic nonconvex optimization," *IEEE Trans. Signal Process.*, vol. 66, no. 22, pp. 5941–5955, Nov. 2018.
- [19] S. M. Kay, *Fundamentals of Statistical Signal Processing: Estimation Theory*. Upper Saddle River, NJ, USA: Prentice-Hall, Inc., 1993.
- [20] K. Yang, T. Jiang, Y. Shi, and Z. Ding, "Federated learning via over-the-air computation," *IEEE Trans. Wireless Commun.*, vol. 19, no. 3, pp. 2022–2035, 2020.
- [21] T. T. Vu, D. T. Ngo, M. N. Dao, S. Durrani, and R. H. Middleton, "Spectral and energy efficiency maximization for content-centric C-RANs with edge caching," *IEEE Trans. Commun.*, vol. 66, no. 12, pp. 6628–6642, Dec. 2018.
- [22] T. T. Vu, D. T. Ngo, M. N. Dao, S. Durrani, D. H. N. Nguyen, and R. H. Middleton, "Energy efficiency maximization for downlink cloud radio access networks with data sharing and data compression," *IEEE Trans. Wireless Commun.*, vol. 17, no. 8, pp. 4955–4970, Aug. 2018.
- [23] S. Boyd and L. Vandenberghe, *Convex Optimization*. New York, NY: Cambridge University Press, 2004.
- [24] V. D. Nguyen, T. Q. Duong, H. D. Tuan, O. S. Shin, and H. V. Poor, "Spectral and energy efficiencies in full-duplex wireless information and power transfer," *IEEE Trans. Commun.*, vol. 65, no. 5, pp. 2220–2233, May 2017.
- [25] V.-D. Nguyen, H. V. Nguyen, C. T. Nguyen, and O. Shin, "Spectral efficiency of full-duplex multi-user system: Beamforming design, user grouping, and time allocation," *IEEE Access*, vol. 5, pp. 5785–5797, 2017.
- [26] B. R. Marks and G. P. Wright, "A general inner approximation algorithm for nonconvex mathematical programs," *Operations Research*, vol. 26, no. 4, pp. 681–683, 1978.
- [27] E. Che, H. D. Tuan, and H. H. Nguyen, "Joint optimization of cooperative beamforming and relay assignment in multi-user wireless relay networks," *IEEE Trans. Wireless Commun.*, vol. 13, no. 10, pp. 5481–5495, Oct. 2014.
- [28] U. Rashid, H. D. Tuan, H. H. Kha, and H. H. Nguyen, "Joint optimization of source precoding and relay beamforming in wireless MIMO relay networks," *IEEE Trans. Commun.*, vol. 62, no. 2, pp. 488–499, Feb. 2014.
- [29] H. S. Dhillon, R. K. Ganti, and J. G. Andrews, "Modeling non-uniform UE distributions in downlink cellular networks," *IEEE Wireless Commun. Lett.*, vol. 2, no. 3, pp. 339–342, Jun. 2013.
- [30] E. Björnson and L. Sanguinetti, "Making cell-free massive MIMO competitive with MMSE processing and centralized implementation," *IEEE Trans. Wireless Commun.*, vol. 19, no. 1, pp. 77–90, Jan. 2020.